JOURNAL OF THEORETICAL AND APPLIED MECHANICS
62, 3, pp. 637-649, Warsaw 2024
https://doi.org/10.15632/jtam-pl/191234

COUPLING EFFECT OF HOLE ENLARGEMENT AND DIFFUSION IN THE GROUTING PROCESS IN A WEAK STRATUM BASED ON ANALYTICAL RESEARCH

Zenghui Zhao

College of Energy and Mining Engineering, Shandong University of Science and Technology, Qingdao, China; and State Key Laboratory of Mining Disaster Prevention and Control Co-founded by Shandong Province and the Ministry of Science and Technology, Shandong University of Science and Technology, Qingdao China

Zhe Meng

College of Energy and Mining Engineering, Shandong University of Science and Technology, Qingdao, China

Longfei Li

College of Energy and Mining Engineering, Shandong University of Science and Technology, Qingdao, China; and State Key Laboratory of Mining Disaster Prevention and Control Co-founded by Shandong Province and the Ministry of Science and Technology, Shandong University of Science and Technology, Qingdao China
correspondinc author, e-mail: lilongfei@sdust.edu.cn

Canlin Li, Peng Yang

College of Energy and Mining Engineering, Shandong University of Science and Technology, Qingdao, China

According to the tail grouting of a double shield TBM tunnel in a soft stratum, the spherical hole model with small and large diffusion radius were established respectively considering the slurry diffusion and slurry displacement effect in the grouting compaction stage. Analytical solutions of the spherical hole expansion stress and displacement field under the hole expansion-diffusion coupling effect are deduced. The interaction among plastic zone radius, reaming radius, initial radius of the spherical hole, and the seepage radius were analyzed. The results show that the larger the seepage pressure of grouting, the smaller the plastic radius. The larger the reaming radius is, the larger the plastic zone radius is. When the reaming radius reaches a certain value, the plastic radius tends to be stable, and the smaller the grouting seepage pressure, the earlier it tends to be stable. The above conclusions have important guiding significance for optimizing grouting parameters in weak strata.

Keywords: weak stratum, shielding, grouting, reaming diffusion, coupling mechanical effect

1. Introduction

The shield construction is widely used in urban rail transit engineering due to its small disturbance to the environment and high speed. However, many urban subway lines pass through prosperous areas, the underground pipelines are crisscrossed, the ground buildings are complex and changeable, and the construction environment is extremely harsh. The shield construction can easily cause uneven subsidence of the stratum, resulting in surface subsidence and building cracking (Epel *et al.*, 2021; Khetwal *et al.*, 2020; Han *et al.*, 2022). As the main method of shield backfilling, the grouting can effectively control deformation of the formation and prevent uneven stress on the segment. However, if the grouting effect is not good, the segment will float,

be damaged, and the surface will rise or sink. Therefore, revealing the mechanical mechanism of shield grouting in weak strata is of great significance to reduce the shield disturbance in weak strata and reduce the surface subsidence and tunnel deformation.

The shield backfill grouting can be divided into four stages: grouting filling, infiltration, compaction and splitting. Regarding the diffusion effect of grouting, Bezuijen and Talmon (2004) and Bezuijen *et al.* (2004) conducted on-site monitoring research and analyzed in detail the slurry diffusion process and the changes in slurry pressure at different stages. Based on the Navier--Stokes equation, Mu *et al.* (2019) established a water glass slurry diffusion model considering the coupling between the slurry and fracture. Boschi *et al.* (2020) studied the interaction between soil particles and grout during grouting from the perspective of meso-mechanics. Zhou *et al.* (2021) established diffusion models for a single-hole and porous grouting based on fractal geometry and seepage effects. Liu *et al.* (2021) revealed the fluid motion law of a synchronous grouting along the unconventional path in the shield tail gap, and obtained the axial and longitudinal pressure distribution patterns. Li *et al.* (2020) proposed the SDS numerical simulation method considering temporal and spatial evolution factors of slurry viscosity, and studied the diffusion law of water glass slurry in cracks under different dynamic water conditions. Xu *et al.* (2021) developed a simulator that could simulate the whole process of grouting reinforcement based on the numerical manifold method.

In the late stage of grouting diffusion, the slurry around the hole has initially coagulated. When the grouting pressure continues to increase, the grouting enters the grouting compaction stage. Squeezing and compacting causes the phenomenon of hole expansion at the orifice. In view of the grouting reaming effect, Li *et al.* (2019) established an improved compaction grouting model considering three-dimensional shear failure to predict the ultimate grouting pressure of compaction grouting. Shrivastava *et al.* (2017) considered grouting compaction as an expansion process of a cylindrical cavity in a finite medium, and provided its analytical solution. Pachen *et al.* (2005) studied the mechanism and effectiveness of medium pressure grouting in loose filled sand through model experiments. El-Kelesh *et al.* (2012) explored the effects of soil parameters, soil compression rate, replacement rate, and injection sequence on the grouting effect of grouting compaction through on-site experiments. Wang *et al.* (2015) conducted numerical simulations of radial expansion and uplift caused by grouting compaction in noncohesive soil. Wang and Zheng (2022) used the pore fluid diffusion/stress coupling analysis method to simulate the grouting compaction process of two on-site tests, and conducted parameter studies on the uplift and settlement caused by grouting and tunnel excavation. Wu *et al.* (2022) considered the compaction effect of grouting under the condition of soil unloading, and established a compaction grouting model considering the effect of soil unloading. Nishimura *et al.* (2011) demonstrated the importance of stress changes in increasing liquefaction resistance by simulating the grouting compaction process in a geocentrifuge.

In the grouting diffusion stage, the pore water in the formation has been displaced within a certain range as the slurry seeps and diffuses into the formation. The formation already contains slurry at this time, and the influence of slurry diffusion on expansion should not be ignored when analyzing the grouting compaction. Most of the scholars' research on the slurry infiltration diffusion and grouting compaction is idealized to separate the grouting stage, but in fact, seepage, compaction and splitting often occur simultaneously in the grouting process, and various stages of grouting are mutually coupled. The existing research rarely considers the interaction between the grouting compaction and grouting diffusion. Therefore, in this paper, considering the slurry diffusion-compaction coupling effect, analytical formulas of stress field and displacement fields in the elastic-plastic zone of soil around the hole are derived, and the effects of groundwater seepage and slurry diffusion radius on the reaming pressure and plastic zone radius are analyzed.

2. Grouting diffusion-compact spherical hole model

The mechanical effect of grouting is manifested in two aspects (Vesić *et al.*, 2021): one is the reaming effect of the grouting hole under the grouting pressure P_k; the other is the diffusion effect of the grout in the formation under the seepage pressure P_j. Assuming that P_w is the pore water pressure, the final reaming radius is r_0. The slurry diffusion radius is r_c, and slurry seepage field is shown in Fig. 1.

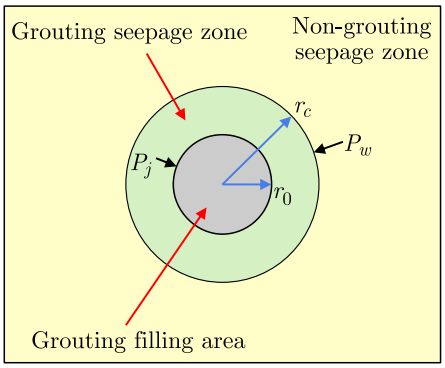

Fig. 1. Seepage field of slurry diffusion

When P_k is small, the soil around the hole has only elastic deformation. When P_k reaches a certain value, the soil will produce plastic deformation, forming a grouting seepage plastic zone. If P_k continues to increase, the plastic zone radius will exceed the slurry diffusion radius to form a plastic zone without grouting seepage. To this end, the analytical model shown in Fig. 2 has been established. It has been assumed that the in-situ stress is P_0, and the plastic zone radius is r_p. When $r_c < r_p$, the plastic zone of the surrounding rock is divided into two regions, namely the grouting seepage plastic zone and the non-grouting seepage plastic zone, which is defined as a small diffusion radius model. When $r_c > r_p$, the plastic zone is the grouting seepage plastic zone, which can be considered as $r_c = r_p$ and defined as the large diffusion radius model.

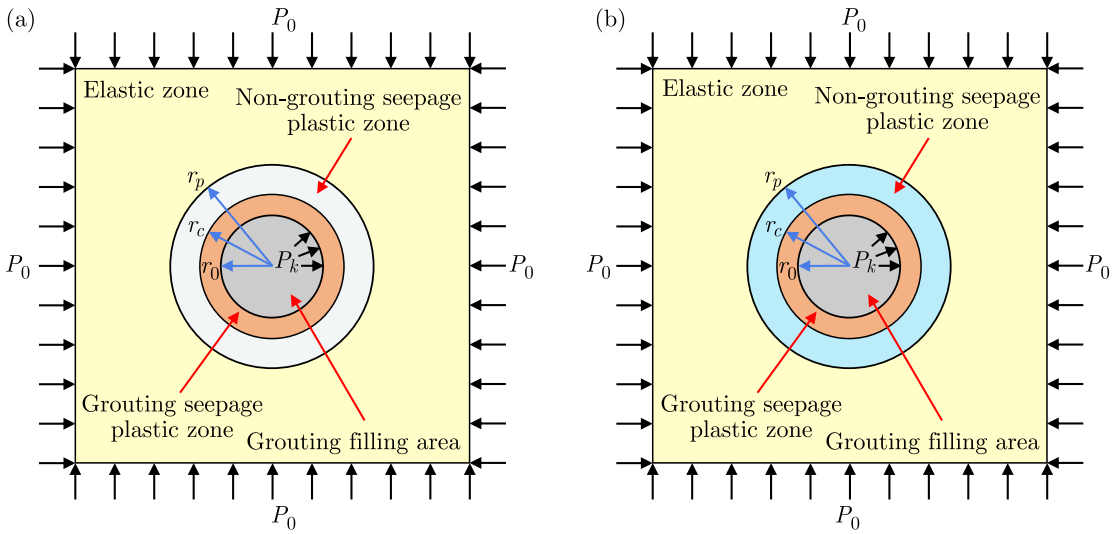

Fig. 2. Coupling model of grouting considering the reaming-diffusion effect: (a) small diffusion radius model, (b) large diffusion radius model

For convenience in analysis, the following assumptions are made:

(1) The stratum is regarded as isotropic and compressible, the compressibility of the slurry is ignored, and the influence of self-weight is not considered;

(2) The slurry diffusion mode is hemispherical diffusion, and the diffusion process follows Darcy's law;
(3) The change of formation permeability during the diffusion process and the influence of slurry diffusion on formation properties are ignored.

3. Analytical solutions of the coupled effect of expansion and diffusion during grouting

3.1. Basic formula

Stress and strain take pressure as positive and tension as negative, considering the influence of grouting seepage and pore water pressure. The spherically symmetric equilibrium differential equation can be uniformly expressed as

$$\frac{\mathrm{d}\sigma_r}{\mathrm{d}r} + 2\frac{\sigma_r - \sigma_\theta}{r} + \frac{\mathrm{d}P_f}{\mathrm{d}r} = 0 \tag{3.1}$$

where σ_r and σ_θ are stresses in the radial and circumferential directions, and P_f is fluid pressure.

The geometric equation is

$$\varepsilon_r = -\frac{\mathrm{d}u_r}{\mathrm{d}r} \qquad \varepsilon_\theta = -\frac{u_r}{r} \tag{3.2}$$

where ε_r and θ are strains in the radial and circumferential directions, u_r is radial displacement.

Using the above equation, the spherically symmetric strain coordination equation can be obtained

$$\frac{\mathrm{d}\varepsilon_\theta}{\mathrm{d}r} + \frac{\varepsilon_\theta - \varepsilon_r}{r} = 0 \tag{3.3}$$

Generalized Hooke's law of spherically symmetric problems is used in the elastic region, i.e.

$$\varepsilon_r = -\frac{\sigma_r - 2\nu\sigma_\theta}{E} \qquad \varepsilon_\theta = -\frac{(1-\nu)\sigma_\theta - \nu\sigma_r}{E} \tag{3.4}$$

where E is elastic Young's modulus, and ν is Poisson's ratio.

In the spherically symmetric model, the hoop stress is equal everywhere, and the stress state is the same as that of the pseudo-triaxial test of the rock. Assuming that the formation yielding behavior satisfies the Mohr-Coulomb criterion, it can be expressed as

$$\sigma_\theta = M\sigma_r + \sigma_0 \tag{3.5}$$

where $M = (1+\sin\theta)/(1-\sin\theta)$, $\sigma_0 = 2c\cos\theta/(1-\sin\theta)$, θ is the internal friction angle, c is cohesion.

The dynamic equilibrium is satisfied at the grouting seepage boundary, that is, differential pressure $\Delta P = P_{gm}\big|_{r=r_c} - P_w = 0$. The seepage boundary condition is

$$P_f\Big|_{r=r_0} = P_j \qquad P_f\Big|_{r=r_c} = P_w \qquad P_f\Big|_{r=\infty} = 0 \tag{3.6}$$

The stable seepage equation (Vesić, 1972) is

$$\frac{\partial^2}{P_f}\partial r^2 + \frac{2}{r}\frac{\partial P_f}{\partial r} = 0 \tag{3.7}$$

Solving the above equation and using boundary condition Eq. (3.6), we can get

$$P_f = \begin{cases} \dfrac{r_0 r_c(P_j - P_w)}{(r_c - r_0)r} + \dfrac{r_c P_w - r_0 P_j}{r_c - r_0} & \text{for} \quad r_0 < r < r_c \\ \dfrac{r_c P_w}{r} & \text{for} \quad r > r_c \end{cases} \tag{3.8}$$

3.2. Solution of the spherical hole model with small diffusion radius for grouting

3.2.1. Elastic zone

Let $\sigma_r = \Phi/r$, by substituting it into Eq. (3.1), we can obtain $\sigma_\theta = [\mathrm{d}\Phi/\mathrm{d}r + (\Phi - k_0)/r]/2$, where k is an intermediate constant that can be eliminated later. Substituting Eq. (3.4) into Eq. (3.3) and substituting $\sigma_r = \Phi/r$, $\sigma + \theta = [\mathrm{d}\Phi/\mathrm{d}r + (\Phi - k_0)/r]/2$ into the resulting expression, the control equation of stress definite solution can be obtained as

$$r^2\frac{\mathrm{d}^2\Phi}{\mathrm{d}r^2} + 2r\frac{\mathrm{d}\Phi}{\mathrm{d}r} - 2\Phi = 0 \tag{3.9}$$

Using Eq. (3.9), the general solution of elastic stress can be obtained as

$$\sigma_r = k_1\frac{1}{r^3} + k_2 \qquad \sigma_\theta = -\frac{1}{2}\frac{k_1}{r^3} + k_2 \tag{3.10}$$

where k_1 and k_2 can be determined by the stress boundary conditions.

Assume that the radial stress of the elastic-plastic boundary is P_{yg}, by using $\sigma_r\big|_{r=r_p} = P_{yg}$, $\sigma_r\big|_{r\to\infty} = P_0$, the stress solutions in the elastic zone are available

$$\sigma_{rse} = (P_{yg} - P_0)\Big(\frac{r_p}{r}\Big)^3 + P_0 \qquad \sigma_{\theta se} = -\frac{1}{2}(P_{yg} - P_0)\Big(\frac{r_p}{r}\Big)^3 + P_0 \tag{3.11}$$

By substituting Eqs. (3.11) and $r = r_p$ into Eq. (3.5), the radial stress of the elastic-plastic boundary can be obtained as

$$P_{yg} = \frac{3MP_0 + 2\sigma_0}{2 + M} \tag{3.12}$$

By substituting Eqs. (3.11) into Eq. (3.4) and subtracting the strain generated by the in-situ stress $\varepsilon_0 = P_0(1 - 2\nu)/E$, and then substituting the resulting expression into Eq. (3.2), the displacement solution of elastic zone can be obtained

$$u_{rse} = -(\varepsilon_\theta - \varepsilon_0)r = \frac{r}{4G}(P_{yg} - P_0)\Big(\frac{r_p}{r}\Big)^3 \tag{3.13}$$

3.2.2. Plastic zone

(1) Non-grouting seepage plastic zone

By substituting Eq. (3.5) and the second expression of Eq. (3.8) into Eq. (3.1), and using the boundary condition $\sigma_r\big|_{r=r_p} = P_{yg}$, the stresses in the non-grouting seepage plastic zone can be obtained as

$$\begin{aligned}
\sigma_{rsp} &= \Big(P_{yg} - \frac{r_cP_w}{r_p(1-2M)} + \frac{\sigma_0}{M-1}\Big)\Big(\frac{r}{r_p}\Big)^{2(M-1)} + \frac{r_cP_w}{(1-2M)r} - \frac{\sigma_0}{M-1} \\
\sigma_{\theta sp} &= M\Big(P_{yg} - \frac{r_cP_w}{r_p(1-2M)} + \frac{\sigma_0}{M-1}\Big)\Big(\frac{r}{r_p}\Big)^{2(M-1)} + \frac{Mr_cP_w}{(1-2M)r} - \frac{\sigma_0}{M-1}
\end{aligned} \tag{3.14}$$

At the grouting seepage boundary, the radial stress is

$$\sigma_{rsp}\Big|_{r=r_c} = \Big(P_{yg} - \frac{r_cP_w}{r_p(1-2M)} + \frac{\sigma_0}{M-1}\Big)\Big(\frac{r_c}{r_p}\Big)^{2(M-1)} + \frac{P_w}{1-2M} - \frac{\sigma_0}{M-1} \tag{3.15}$$

Using the associated flow criteria

$$\mathrm{d}\varepsilon_{ij}^p = \mathrm{d}\lambda\frac{\partial f}{\partial\sigma_{ij}} \tag{3.16}$$

where ε_{ij}^{p} is the plastic strain tensor, substituting Eq. (3.5) into Eqs. (3.14), we can get

$$\mathrm{d}\varepsilon_r^p = \mathrm{d}\lambda\frac{\partial f}{\partial\sigma_r} = \mathrm{d}\lambda \qquad \mathrm{d}\varepsilon_\theta^p = \mathrm{d}\lambda\frac{\partial f}{\partial\sigma_\theta} = -M\mathrm{d}\lambda \tag{3.17}$$

It can be obtained from the above equation

$$\frac{\mathrm{d}\varepsilon_r^p}{\mathrm{d}\varepsilon_\theta^p} = -\frac{1}{M} \tag{3.18}$$

The strain relationship in the plastic zone is

$$\varepsilon_r = \varepsilon_r^e + \varepsilon_r^p \qquad \varepsilon_\theta = \varepsilon_\theta^e + \varepsilon_\theta^p \tag{3.19}$$

Substituting Eqs. (3.18) and (3.18) into Eq. (3.3), one gets

$$\frac{\mathrm{d}\varepsilon_\theta^p}{\mathrm{d}r} + \Big(1+\frac{1}{M}\Big)\frac{\varepsilon_\theta^p}{r} + \frac{\varepsilon_\theta^e - \varepsilon_r^e}{r} + \frac{\mathrm{d}\varepsilon_\theta^e}{\mathrm{d}r} = 0 \tag{3.20}$$

Substituting Eqs. (3.14) into Eq. (3.4), the elastic strain in the plastic zone is

$$\begin{aligned}
\varepsilon_{rsp}^e &= \frac{2\nu M-1}{E}\left(\Big(P_{yg} - \frac{r_cP_w}{r_p(1-2M)} + \frac{\sigma_0}{M-1}\Big)\Big(\frac{r}{r_p}\Big)^{2(M-1)} + \frac{r_cP_w}{(1-2M)r}\right) \\
&\quad + \frac{(1-2\nu)\sigma_0}{E(M-1)} \\
\varepsilon_{\theta sp}^e &= \frac{\nu-(1-\nu)M}{E}\left(\Big(P_{yg} - \frac{r_cP_w}{r_p(1-2M)} + \frac{\sigma_0}{M-1}\Big)\Big(\frac{r}{r_p}\Big)^{2(M-1)} + \frac{r_cP_w}{(1-2M)r}\right) \\
&\quad + \frac{(1-2\nu)\sigma_0}{E(M-1)}
\end{aligned} \tag{3.21}$$

Substituting Eqs. (3.21) into Eq. (3.20) and using the boundary condition $\varepsilon_{\theta sp}^{p}\big|_{r=r_p} = 0$, the circumferential plastic strain can be written as

$$\begin{aligned}
\varepsilon_{\theta sp}^p &= -\frac{M(1+2M)(1-M)(1-\nu)}{2M^2-M+1}\Big(P_{yg} - \frac{r_cP_w}{r_p(1-2M)} + \frac{\sigma_0}{M-1}\Big)\Big(\frac{r}{r_p}\Big)^{2(M-1)} \\
&\quad - \frac{M(1-2\nu M)r_cP_w}{(1-2M)r} + \frac{M(1-2\nu M)r_cP_w}{(1-2M)r_p}\Big(\frac{r_p}{r}\Big)^{1+\frac{1}{M}} \\
&\quad + \frac{M(1+2M)(1-M)(1-\nu)}{2M^2-M+1}\Big(P_{yg} - \frac{r_cP_w}{r_p(1-2M)} + \frac{\sigma_0}{M-1}\Big)\Big(\frac{r_p}{r}\Big)^{1+\frac{1}{M}}
\end{aligned} \tag{3.22}$$

Using Eq. (3.22), the plastic strain at the junction of the two plastic regions can be obtained

$$\begin{aligned}
\varepsilon_{\theta sp}^p\Big|_{r=r_c} &= -\frac{M(1+2M)(1-M)(1-\nu)}{2M^2-M+1}\Big(P_{yg} - \frac{r_cP_w}{r_p(1-2M)} + \frac{\sigma_0}{M-1}\Big)\Big(\frac{r_c}{r_p}\Big)^{2(M-1)} \\
&\quad - \frac{M(1-2\nu M)P_w}{1-2M} + \frac{M(1-2\nu M)P_w}{1-2M}\Big(\frac{r_p}{r_c}\Big)^{\frac{1}{M}} \\
&\quad + \frac{M(1+2M)(1-M)(1-\nu)}{2M^2-M+1}\Big(P_{yg} - \frac{r_cP_w}{r_p(1-2M)} + \frac{\sigma_0}{M-1}\Big)\Big(\frac{r_p}{r_c}\Big)^{1+\frac{1}{M}}
\end{aligned} \tag{3.23}$$

Similar to Eq. (3.13), combining Eqs. (3.2), (3.19), (3.21) and (3.22), the displacement solution of non-grouting seepage plastic zone can be obtained

$$u_{rsp} = -(\varepsilon_\theta - \varepsilon_0)r \tag{3.24}$$

(2) Grouting seepage plastic zone

By substituting Eq. (3.5) and the first expression of Eq. (3.8) into Eq. (3.1) and using boundary condition Eq. (3.15), the stresses in the grouting seepage plastic zone can be obtained as

$$\begin{aligned}\sigma_{rsg} &= \Big(P_{yg} - \frac{r_c P_w}{r_p(1-2M)} + \frac{\sigma_0}{M-1}\Big)\Big(\frac{r}{r_p}\Big)^{2(M-1)} \\ &\quad + \Big(\frac{P_w}{1-2M} - \frac{r_0(P_j-P_w)}{(1-2M)(r_c-r_0)}\Big)\Big(\frac{r}{r_c}\Big)^{2(M-1)} + \frac{r_0 r_c(P_j-P_w)}{(r_c-r_0)(1-2M)r} - \frac{\sigma_0}{M-1} \\ \sigma_{\theta sg} &= M\Big(P_{yg} - \frac{r_c P_w}{r_p(1-2M)} + \frac{\sigma_0}{M-1}\Big)\Big(\frac{r}{r_p}\Big)^{2(M-1)} \\ &\quad + M\Big(\frac{P_w}{1-2M} - \frac{r_0(P_j-P_w)}{(1-2M)(r_c-r_0)}\Big)\Big(\frac{r}{r_c}\Big)^{2(M-1)} + \frac{M r_0 r_c(P_j-P_w)}{(r_c-r_0)(1-2M)r} - \frac{\sigma_0}{M-1}\end{aligned} \tag{3.25}$$

Substituting Eqs. (3.25) into Eq. (2.4), the elastic strain in the plastic zone is obtained as

$$\begin{aligned}\varepsilon^e_{rsg} &= \frac{2\nu M-1}{E}\Bigg(\Big(P_{yg} - \frac{r_c P_w}{r_p(1-2M)} + \frac{\sigma_0}{M-1}\Big)\Big(\frac{r}{r_p}\Big)^{2(M-1)} + \frac{r_0 r_c(P_j-P_w)}{(r_c-r_0)(1-2M)r} \\ &\quad + \Big(\frac{P_w}{1-2M} - \frac{r_0(P_j-P_w)}{(1-2M)(r_c-r_0)}\Big)\Big(\frac{r}{r_c}\Big)^{2(M-1)}\Bigg) + \frac{(1-2\nu)\sigma_0}{E(M-1)} \\ \varepsilon^e_{\theta sg} &= \frac{\nu-(1-\nu)M}{E}\Bigg(\Big(P_{yg} - \frac{r_c P_w}{r_p(1-2M)} + \frac{\sigma_0}{M-1}\Big)\Big(\frac{r}{r_p}\Big)^{2(M-1)} + \frac{r_0 r_c(P_j-P_w)}{(r_c-r_0)(1-2M)r} \\ &\quad + \Big(\frac{P_w}{1-2M} - \frac{r_0(P_j-P_w)}{(1-2M)(r_c-r_0)}\Big)\Big(\frac{r}{r_c}\Big)^{2(M-1)}\Bigg) + \frac{(1-2\nu)\sigma_0}{E(M-1)}\end{aligned} \tag{3.26}$$

Substituting Eq. (3.26) into Eq. (3.20) and using the boundary condition $\varepsilon^p_{\theta sg}\big|_{r=r_c} = \varepsilon^p_{\theta sp}\big|_{r=r_c}$, i.e. Eq. (3.23), the circumferential plastic strain can be written as

$$\begin{aligned}\varepsilon^p_{\theta sg} &= \frac{M(1+2M)(1-M)(1-\nu)}{2M^2-M+1}\Bigg[\Big(P_{yg} - \frac{r_c P_w}{r_p(1-2M)} \\ &\quad + \frac{\sigma_0}{M-1}\Big)\Bigg(\Big(\frac{r_p}{r}\Big)^{1+\frac{1}{M}} - \Big(\frac{r}{r_p}\Big)^{2(M-1)}\Bigg) \\ &\quad + \Big(\frac{P_w}{1-2M} - \frac{r_0(P_j-P_w)}{(1-2M)(r_c-r_0)}\Big)\Bigg(\Big(\frac{r_c}{r}\Big)^{1+\frac{1}{M}} - \Big(\frac{r}{r_c}\Big)^{2(M-1)}\Bigg)\Bigg] \\ &\quad - \frac{M(1-2\nu M)r_0 r_c(P_j-P_w)}{(r_c-r_0)(1-2M)r} \\ &\quad + \frac{M(1-2\nu M)}{1-2M}\Bigg(P_w\Big(\frac{r_p}{r_c}\Big)^{\frac{1}{M}} - P_w + \frac{r_0(P_j-P_w)}{(r_c-r_0)}\Bigg)\Big(\frac{r_c}{r}\Big)^{1+\frac{1}{M}}\end{aligned} \tag{3.27}$$

Similar to Eq. (3.13), using Eqs. (3.2), (3.19), (3.26) and (3.27), the relative displacement can be obtained as

$$u_{rsg} = -(\varepsilon_\theta - \varepsilon_0)r \tag{3.28}$$

When the injected stratum is sandy soil or a soft stratum with similar physical properties to sandy soil, the diffusion radius considering the displacement effect can be calculated by the following equation (Ye *et al.*, 2022)

$$r_c = r_0 + r_c' = 3\frac{tK(P_k - P_w)}{\phi[(\mu_g - \mu_w)r_c' + \mu_w l_w]} \tag{3.29}$$

where r_c' is diffusion radius under displacement, μ_g, μ_w are slurry viscosity and groundwater viscosity, K is permeability, ϕ is soil porosity, P_w is groundwater pressure at l_w, t is grouting time, r_0 is reaming radius.

3.3. Grouting compaction-solution of the spherical hole model with a large diffusion radius

At this time, there is only a grouting seepage plastic zone in the plastic zone of the surrounding rock. It can be considered that $r_c = r_p$, then the stress boundary condition is

$$\sigma_r\Big|_{r=r_0} = P_k \tag{3.30}$$

Similar to the above derivation, the stress solution in the plastic zone can be obtained

$$\begin{aligned}
\sigma_{rg} &= \Big(P_k - \frac{r_0 r_c(P_j - P_w)}{r_0(r_c - r_0)(1-2M)} + \frac{\sigma_0}{M-1}\Big)\Big(\frac{r}{r_0}\Big)^{2(M-1)} + \frac{r_0 r_c(P_j - P_w)}{(r_c - r_0)(1-2M)r} - \frac{\sigma_0}{M-1} \\
\sigma_{\theta lg} &= M\Big(P_k - \frac{r_0 r_c(P_j - P_w)}{r_0(r_c - r_0)(1-2M)} + \frac{\sigma_0}{M-1}\Big)\Big(\frac{r}{r_0}\Big)^{2(M-1)} + \frac{M r_0 r_c(P_j - P_w r)}{(r_c - r_0)(1-2M)r} - \frac{\sigma_0}{M-1}
\end{aligned} \tag{3.31}$$

And the plastic zone strain solution can be expressed as

$$\begin{aligned}
\varepsilon_{rlg}^e &= \frac{2\nu M - 1}{E}\Bigg(\Big(P_k - \frac{r_c(P_j - P_w)}{(r_c - r_0)(1-2M)} + \frac{\sigma_0}{M-1}\Big)\Big(\frac{r}{r_0}\Big)^{2(M-1)} \\
&\quad + \frac{r_0 r_c(P_j - P_w)}{(r_c - r_0)(1-2M)r}\Bigg) + \frac{(1-2\nu)\sigma_0}{E(M-1)} \\
\varepsilon_{\theta lg}^e &= \frac{\nu - (1-\nu)M}{E}\Bigg(\Big(P_k - \frac{r_c(P_j - P_w)}{(r_c - r_0)(1-2M)} + \frac{\sigma_0}{M-1}\Big)\Big(\frac{r}{r_0}\Big)^{2(M-1)} \\
&\quad + \frac{r_0 r_c(P_j - P_w)}{(r_c - r_0)(1-2M)r}\Bigg) + \frac{(1-2\nu)\sigma_0}{E(M-1)} \\
\varepsilon_{\theta lg}^p &= -\frac{M(1+2M)(1-M)(1-\nu)}{2M^2 - M + 1}\Big(P_k - \frac{r_c(P_j - P_w)}{(r_c - r_0)(1-2M)} + \frac{\sigma_0}{M-1}\Big)\Big(\frac{r}{r_0}\Big)^{2(M-1)} \\
&\quad - \frac{M(1-2\nu M)r_0 r_c(P_j - P_w)}{(r_c - r_0)(1-2M)r} + \frac{M(1-2\nu M)r_0(P_j - P_w)}{(r_c - r_0)(1-2M)}\Big(\frac{r_c}{r}\Big)^{1+\frac{1}{M}} \\
&\quad + \frac{M(1+2M)(1-M)(1-\nu)}{2M^2 - M + 1}\Big(P_k - \frac{r_c(P_j - P_w)}{(r_c - r_0)(1-2M)} + \frac{\sigma_0}{M-1}\Big)\Big(\frac{r_c}{r_0}\Big)^{2(M-1)}\Big(\frac{r_c}{r}\Big)^{1+\frac{1}{M}}
\end{aligned} \tag{3.32}$$

Similar to Eq. (3.13), using Eqs. (3.2), (3.19) and (3.32), the displacement solution can be obtained

$$u_{rlg} = -(\varepsilon_\theta - \varepsilon_0)r \tag{3.33}$$

4. Model discussion

4.1. Large diffusion radius model

Taking the physical and mechanical parameters of the formation as shown in Table 1, the relationship between the reaming radius and the plastic zone radius is analyzed.

Table 1. Physical and mechanical parameters of strata

Elastic Young's modulus E [MPa]	Diffusion radius r_c [m]	Porosity K	Poisson's ratio μ	Initial geostress P_0 [kPa]	Internal friction angle θ [°]	Cohesion c [kPa]	Initial grouting radius r_k [m]
26	1.33	0.3	0.3	100	25	20	0.1

Figure 3 shows the relationship between the reaming radius and the plastic zone radius obtained by using the model in this paper when P_j is 0 kPa, 30 kPa and 50 kPa. The calculation results of the model have a similar change trend to the results of Mei *et al.* (2017), but the upward trend of the results in this paper is relatively slow and the value is small. This is because the results of Mei *et al.* (2017) only consider the effect of the lower grout seepage on the plastic zone of the surrounding rock. In fact, in the grouting diffusion stage, the grout has penetrated and diffused into the formation, which has a strengthening effect on the formation, which reduces the plastic zone of the surrounding rock. The larger P_j is, the smaller the plastic radius is, and the slurry has a certain improvement on the surrounding rock during the diffusion stage.

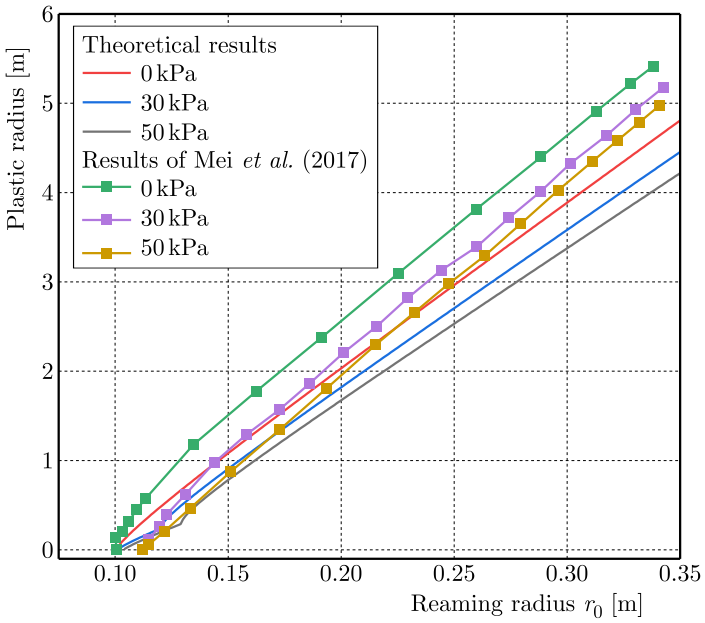

Fig. 3. Comparison of the theoretical calculation of seepage diffusion in grouting with Mei *et al.* (2017)

Figure 4a shows the relationship between the reaming pressure and the reaming radius. It can be seen that the reaming pressure increases rapidly in the range of the reaming radius of 0 m-1 m, and the slurry diffusion has a certain influence on the reaming pressure. When P_j is 0 kPa, 30 kPa and 50 kPa, respectively, the reaming pressure is stable at 4.38 MPa, 4.22 MPa and 4.1 MPa. Figure 4b shows the effect of the reaming radius r_0 on r_p/r_0. The plastic zone radius increases with an increase in reaming radius. It increases rapidly at the beginning of reaming, then the growth trend is slow, and finally reaches a steady state. r_p/r_0 finally stabilized between 15 and 17, while increasing P_j would make the ratio decrease.

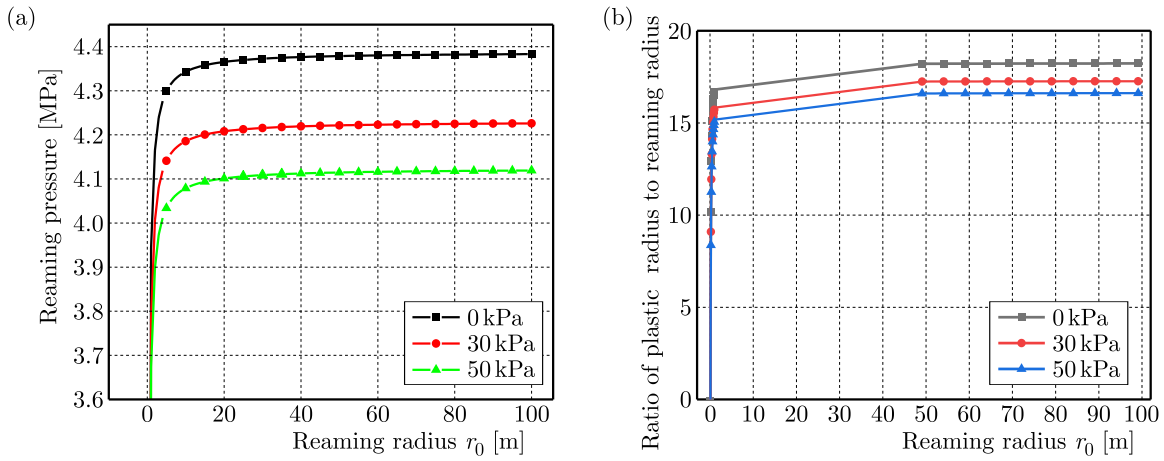

Fig. 4. (a) Expansion pressure curve and (b) influence of reaming on the ratio of plastic zone radius

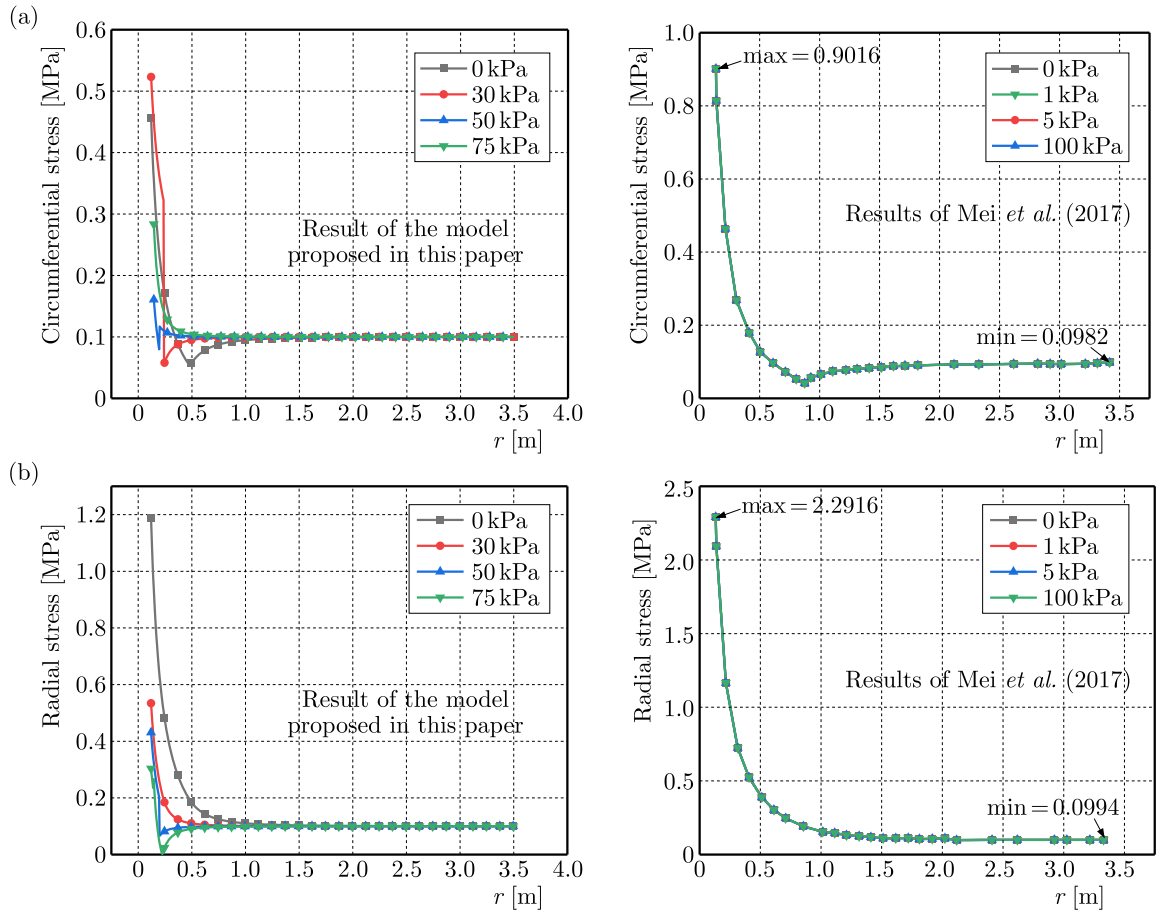

Fig. 5. Stress distribution curve along the radial direction without considering the displacement effect: (a) circumferential stress, (b) radial stress

Figure 5 shows the stress evolution law under different grouting infiltration pressures in the hole when the reaming radius $r_0 = 0.12$ m. The larger the P_j, the smaller the plastic zone. When the P_j increases from 0 to 75 kPa, the radius of the plastic zone decreases from 0.48 m to 0.143 m. This is because after the slurry penetrates and diffuses, it has a certain reinforcement effect on the soil, so that the plastic zone of the surrounding rock is reduced to a certain extent in the compaction stage. Compared with the literature (Mei *et al.*, 2017), it is found that the

two change trends are consistent, but after considering the grouting diffusion stage, the stress in the plastic zone of the surrounding rock decreases compared with the stage without considering the slurry diffusion, and the stress reaches the minimum value at the radius of the plastic zone. Therefore, the slurry diffusion has some influence on the grouting compaction stage.

4.2. Small diffusion radius model

If the displacement effect is not considered, the diffusion radius is only related to the permeability. If the displacement effect is considered, there are many factors affecting the permeability radius, and the grouting pressure will also affect the permeability radius. In the following analysis, the displacement effect is considered, and the calculation parameters at $l_w = 5\,\text{m}$ are selected, as shown in Table 2, and the formation-related parameters are shown in Table 1. Using the formula in Section 3, it can be obtained that when $P_j = 0\,\text{kPa}$, $r_c = 5.45\,\text{m}$; when $P_j = 30\,\text{kPa}$, $r_c = 5.66\,\text{m}$; when $P_j = 50\,\text{kPa}$, $r_c = 5.66\,\text{m}$.

Table 2. Grouting calculation parameters considering displacement effect

Water pressure P_w [MPa]	Porosity ϕ	Water viscosity μ_w [Pa·s]	Grouting time t [s]	Slurry viscosity μ_g [Pa·s]	Permeability coefficient m [cm/s]	Initial grouting radius r_k [m]	Grouting time [min]
0.05	0.3	0.00101	3000	0.0047	0.03	0.1	50

Figure 6 shows the effect of the reaming radius on plastic radius under the displacement effect. The grouting plastic zone is still nonlinear, and the non-grouting plastic zone is greatly affected by the grouting pressure. The greater the grouting pressure, the greater the penetration radius. With an increase in the reaming radius, the ratio of the plastic zone radius to the reaming radius finally approaches a constant, and this constant gradually decreases with an increase in the grouting pressure. This is because when the grouting pressure is constant, with an increase in the grouting osmotic pressure, the volume of the grout entering the soil increases, and the disturbed zone of the surrounding rock continuously expands, resulting in an increase in the radius of the plastic zone. When the reaming radius reaches a certain value, the plastic radius tends to be stable, and the smaller P_j is, the sooner it tends to be stable, which is relatively consistent with the actual situation of grouting.

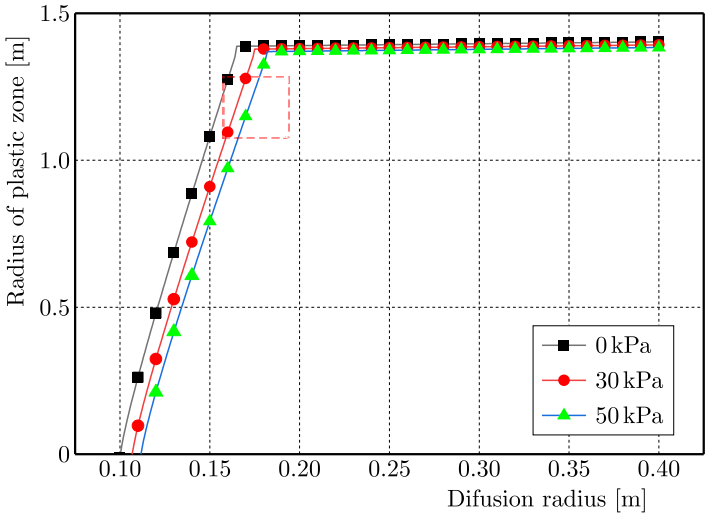

Fig. 6. Effect of grounting diffusion on plastic radius under the displacement effect

Comparing Figs. 4b and 6, it can be seen that when the displacement effect is not considered, the grouting pressure has little effect on the radius of the plastic zone and cannot play a decisive role. When the displacement effect of groundwater and grout is considered, the reaming radius and the plastic zone radius in the non-grouting plastic zone show a nonlinear relationship. With a gradual increase of the reaming radius, the radius of the plastic zone shows a trend of rapid growth at first, and then a slow growth. At the same time, with an increase in the grouting pressure, the radius of plastic zone does not have a large gap, so the grouting pressure does not play a decisive role in the change of the radius of the plastic zone.

5. Conclusion

Considering the slurry diffusion and slurry displacement effect in the grouting compaction stage, a diffusion-compaction model of shield backfill grouting was established. The stress and displacement fields of spherical hole expansion problem considering the coupling effect of reaming and diffusion in grouting process were established. The main conclusions are as follows:

- When the displacement effect of groundwater and grouting slurry is considered, the surrounding rock stress is the same as when only the slurry diffusion is considered, but the displacement of the plastic zone is significantly reduced, and the stress has a minimum point, which corresponds to the radius of the plastic zone.
- The grouting pressure and reaming radius have influence on the radius of plastic zone during the seepage and diffusion of slurry. The larger P_j is, the smaller the plastic radius is, and the larger the cavity expansion radius is, the larger the radius of plastic zone is. When the cavity expansion radius reaches a certain value, the plastic radius tends to be stable, and the smaller P_j is, the sooner it tends to be stable, which is relatively consistent with the actual situation of shield backfill grouting.
- The groundwater flow is more complex. In order to facilitate the analysis, this paper simplifies the groundwater to laminar flow and does not consider turbulence. Therefore, further research on this issue should be conducted in the future.

Acknowledgements
This work was supported by Shandong Provincial Natural Science Foundation (No. ZR2023ME086).

References

1. Bezuijen A., Talmon A., 2004, Grout pressures around a tunnel lining, influence of grout consolidation and loading on lining, *Tunnelling. a Decade of Progress. GeoDelft 1995-2005*, 109-114
2. Bezuijen A., Talmon A., Kaalberg F.J., Plugge R., 2004, Field measurements of grout pressures during tunnelling of the Sophia Rail Tunnel, *Soils and Foundations*, **44**, 1, 39-48.
3. Boschi K., Di Prisco C.G., Ciantia M.O., 2020, Micromechanical investigation of grouting in soils, *International Journal of Solids and Structures*, **187**, 121-132
4. El-Kelesh Adel M., Matsui T., 2012, Effect of soil and grouting parameters on the effectiveness of compaction grouting, *Grouting and Ground Treatment*, 1056-1070
5. Epel T., Mooney M.A., Gutierrez M., 2021, The influence of face and shield annulus pressure on tunnel liner load development, *Tunnelling and Underground Space Technology*, **117**, 104096
6. Han X., Liang X., Ye F., Wang X., Chen Z., 2022, Statistics and construction methods for deep TBM tunnels with high geostress: A case study of Qinling Tunnel in Hanjiang-Weihe River Diversion Project, *Engineering Failure Analysis*, **138**, 106301

7. Khetwal A., Rostami J.I., Nelson P., 2020, Investigating the impact of TBM downtimes on utilization factor based on sensitivity analysis, *Tunnelling and Underground Space Technology*, **106**, 103586
8. Li L., Xiang Z.-C., Zou J.-F., Wang F., 2019, An improved model of compaction grouting considering three-dimensional shearing failure and its engineering application, *Geomechanics and Engineering*, **19**, 3, 217
9. Li S., Pan D., Xu Z., Lin P., Zhang Y., 2020, Numerical simulation of dynamic water grouting using quick-setting slurry in rock fracture: the Sequential Diffusion and Solidification (SDS) method, *Computers and Geotechnics*, **122**, 103497
10. Liu J., Li P., Shi L., Fan J., Kou X., Huang D., 2021, Spatial distribution model of the filling and diffusion pressure of synchronous grouting in a quasi-rectangular shield and its experimental verification, *Underground Space*, **6**, 6, 650-664
11. Mei B.X., Yang M., Jia S.H., 2017, Mohr-Coulomb criterion-based theoretical solutions of spherical cavity expansion considering seepage (in Chinese), *Journal of Tongji University (Natural Science)*, **45**, 3, 309-316
12. Mu W., Li L., Yang T., Yu G., Han Y., 2019, Numerical investigation on a grouting mechanism with slurry-rock coupling and shear displacement in a single rough fracture, *Bulletin of Engineering Geology and the Environment*, **78**, 8, 6159-6177
13. Nishimura S., Takehana K., Morikawa Y., Takahashi H., 2011, Experimental study of stress changes due to compaction grouting, *Soils and Foundations*, **51**, 6, 1037-1049
14. Pachen H., Meijers P., Korff M., Maertens J., 2005, Effect of compaction grouting in loosely packed sand on density, *Stand Alone*, **0**, 1241-1244
15. Shrivastava N., Zen K., Shukla S.K., 2017, Modeling of compaction grouting technique with development of cylindrical cavity expansion problem in a finite medium, *International Journal of Geosynthetics and Ground Engineering*, **3**, 4, 40
16. Shukla M., Gottumukkala B., Nagabhushana M.N., Chandra S., Shaw A., Das S., 2021, Design and evaluation of mechanical properties of cement grouted bituminous mixes (CGBM), *Construction and Building Materials*, **269**, 121805
17. Vesić A.S., 1972, Expansion of cavities in infinite soil mass, *Journal of the Soil Mechanics and Foundations Division*, **98**, 3, 265-290
18. Wang D., Xing X., Qu H., Zhang L.M., 2015, Simulated radial expansion and heave caused by compaction grouting in noncohesive soils, *International Journal of Geomechanics*, **15**, 4, 04014069
19. Wang L., Zheng G., 2022, Numerical evaluation of the upheave and soil arching associated with compaction grouting in shield tunneling and loading process, *Tunnelling and Underground Space Technology*, **128**, 104664
20. Wu Y., Zhao C., Zhao C., Liu F., Zhang J., 2022, Modeling of compaction grouting considering the soil unloading effect, *International Journal of Geomechanics*, **22**, 6, 04022061
21. Xu X., Wu Z., Sun H., Weng L., Chu Z., Liu Q., 2021, An extended numerical manifold method for simulation of grouting reinforcement in deep rock tunnels, *Tunnelling and Underground Space Technology*, **115**, 104020
22. Ye F., Qin N., Liang X., Han X.B., Han X., 2022, Microscopic model analysis of shield tunnel backfill grouting based on displacement effect (in Chinese), *Journal of Southwest Jiaotong University*, **57**, 2, 339-345
23. Zhou Z., Wang K., Feng H., Tian Y., Zhu S., 2021, Centrifugal model test of post-grouting pile group in loess area, *Soil Dynamics and Earthquake Engineering*, **151**, 106985

Manuscript received September 21, 2023; accepted for print Marcn 11, 2024